Phenotype Representation and Analysis via Discriminative Atypicality (PRADA) to capture the structural heterogeneity of Autism Spectrum Disorder

Emre Onemli[1], Ahsan Mahmood[1], Omar Azrak[1], Dea Garic[1], Meghan R. Swanson[2], Rebecca Grzadzinski[1], Kattia Mata[1], Mark D. Shen[1], Jessica B. Girault[1], Tanya St. John[3], Juhi Pandey[4], Lonnie Zwaigenbaum[5], Annette M. Estes[3], Audrey M. Shen[6], Stephen R. Dager[3], Robert T. Schultz[4], Kelly N. Botteron[7], Alan C. Evans[8], Jed T. Elison[2], Essa Yacoub[2], Sun Hyung Kim[1], Robert C. McKinstry[7], Guido Gerig[9], Heather C. Hazlett[1], Natasha Marrus[7], Joseph Piven[1], John R. Pruett Jr[7], and Martin Styner[1]

[1] University of North Carolina at Chapel Hill, USA
[2] University of Minnesota, USA
[3] University of Washington, USA
[4] Center for Autism Research, Children's Hospital of Philadelphia, USA
[5] University of Alberta, Canada
[6] Easter Seals UCP, USA
[7] Washington University in St. Louis, USA
[8] McGill University, Canada
[9] New York University, USA

Abstract. Most current neuroimaging analyses in studies of brain disorders assume a homogenous presentation of the disorder such that traditional statistical analysis methods based on Gaussian distributions can be applied. Yet, most brain disorders present with a heterogeneous spectrum of cognitive, behavioral, morphometric as well as functional manifestations. In this paper, we introduce a novel approach called PRADA (Phenotype Representation and Analysis via Discriminant Atypicality) that embraces the heterogeneity of both typical and atypical brain morphometry. This approach employs Multiscale Score Matching Analysis (MSMA), a global and local multiscale out-of-distribution analysis via the gradients of the log density (scores). Combining MSMA and manifold-mapping, we compute a morphospace of brain phenotypes representing deviations from a population of typical subjects. Using these brain phenotypes, disorder-related subtyping can be performed. Furthermore, subject-specific profiles of atypicality can be extracted via Spatial-MSMA and summarized per subtype. We show the application of PRADA to structural MRI data in a study of Autism Spectrum Disorder (ASD). The resulting analysis detects disorder-related subtypes and reveals that subtype-specific structural atypicality correlates with cognitive and behavioral outcomes. These results highlight the potential of PRADA to discover disorder relevant phenotypes.

Keywords: Neuroimaging, Manifold learning, Out-of-distribution, Phenotype learning, Autism Spectrum Disorder, Self-Organizing Map

1 Introduction

Neurodevelopmental disorders (NDDs) are a diverse group of conditions characterized by atypical brain development, leading to cognitive, social, and emotional impairments. NDDs such as autism spectrum disorder (ASD), Down Syndrome (DS), and attention-deficit/hyperactivity disorder (ADHD), are inherently heterogeneous in presentation and neurobiology [14]. For instance, 30% of individuals with ASD also receive an ADHD diagnosis, underscoring the significant overlap and complexity of NDDs [22]. Understanding this variability is crucial for advancing diagnostic methods, personalized interventions, and insights into the shared and unique neural mechanisms underlying these conditions.

Atypicality in NDDs refers to deviations from normative brain structures or functions that influence cognitive, social, or emotional behaviors. These deviations can manifest as differences in brain morphology, connectivity, or regional activity patterns [10]. Structural atypicality is often assessed relative to a control population, enabling the detection of atypical phenotypes through advanced machine learning techniques [26]. By modeling brain morphometry, researchers can identify disorder-specific patterns and subgroups, providing a deeper understanding of the variability of NDDs [11].

Deep learning approaches such as convolutional neural networks (CNNs) have been used to classify atypical brain patterns. For example, Schirrmeister et al. applied CNNs to detect abnormalities in EEG data [18]. While effective for EEG signals, these methods face challenges in handling structural MRI data due to differences in resolution and complexity.

Attribution-based methods identify anomalies by highlighting input features that significantly influence a model's predictions, often using techniques like GradCAM or SHAP for feature importance localization [20]. However, such methods require labeled data and are less effective in unsupervised settings.

Out-of-distribution (OOD) detection has emerged as a powerful tool for identifying deviations from normative populations. It has been widely used in healthcare, fraud detection, and self-driving applications [21]. In the context of neuroimaging, OOD methods offer a structured framework to evaluate how individual brain phenotypes deviate from a learned normative distribution. A variety of OOD computational approaches have been applied to neuroimaging data. Generative models, such as generative adversarial networks (GANs), attempt to reconstruct normative data and detect anomalies based on reconstruction errors. Schlegl et al. used GANs for anomaly detection in medical imaging [19]. However, these methods often fail when anomalies closely resemble normative data or when reconstruction quality is suboptimal for this task.

Projection-based methods embed neuroimaging data into a lower-dimensional space to distinguish normative from atypical patterns. Bergmann et al. introduced a Student-Teacher network, where discrepancies between a larger Teacher

model and a compressed Student model highlight anomalies [1]. Although effective, these methods require careful calibration and lack interpretability in complex neuroimaging data.

Multiscale Score Matching Analysis (MSMA) computes atypicality by analyzing score norms derived from MRI data across multiple noise scales [12]. This approach provides robust anomaly detection for high-dimensional data, such as images, but lacks direct mechanisms for visualizing and interpreting atypicality. Here, we aim to extend MSMA for such a localized interpretation of atypicality on a manifold representing a morphospace of brain structure.

Manifold learning techniques such as t-SNE and UMAP have been extensively applied to neuroimaging data to uncover meaningful low-dimensional representations of brain activity patterns [2, 28]. Gao et al. demonstrated how nonlinear embedding techniques provide insights into the structure of brain phenotypes [6]. However, traditional manifold learning methods suffer from limitations such as lack of adaptability, lack of invertibility, poor global structure representation, and difficulty handling heterogeneous data distributions [24].

Self-organizing maps (SOMs) have been widely applied for robust manifold mapping, clustering, and visualization of neuroimaging data while preserving topological relationships [9]. However, SOMs require predefined map sizes, which limits their flexibility and scalability in complex datasets. Growing Hierarchical Self-Organizing Map (GHSOM) addresses these limitations by dynamically expanding and adding hierarchical layers, enabling a low hyper-parameter-based interpretable representation of data [4, 16]. This adaptability makes GHSOM a promising tool for analyzing neuroimaging data, where structural heterogeneity is a key characteristic.

Building on MSMA and its voxel-wise extension Spatial-MSMA [13], we introduce PRADA (Phenotype Representation and Analysis via Discriminative Atypicality), a novel framework that extracts a morphospace of atypicality for analyzing disorder-related brain phenotypes. PRADA employs GHSOM to create a low-parameter, hierarchy-aware manifold without requiring a predefined map size, improving interpretability. It uniquely integrates MSMA's robust atypicality detection with GHSOM's hierarchical structure to enable visual and quantitative subtype discovery not addressed by existing image-based deep-learning methods. This work presents the following key advancements in the proposed PRADA approach:

- A novel framework called PRADA for discovering the heterogeneity of NDDs by combining atypicality quantification via MSMA and morphospace representation via GHSOM.
- Application of PRADA to structural neuroimaging data, enabling dynamic and hierarchical mapping of brain phenotypes.
- Analyzing the correlation of image atypicality with behavioral assessments to improve our understanding of NDD phenotypes.
- Application of PRADA to a study of ASD illustrating the potential for disorder-relevant subtypes/phenotypes.

Table 1. Subject distribution by dataset, scanner, sex, and age (mean ± std).

Dataset	Prisma Fit	Prisma	MR750	Achieva	Ingenia	Sex: F/M	Total	Age (yrs)
ABCD Train	448	382	162	68	40	603/499	1107	9.51 ± 0.50
HCP-D Train	–	378	–	–	–	193/185	378	12.73 ± 2.85
ABCD Val	50	44	17	7	6	60/65	125	9.48 ± 0.52
HCP-D Val	–	40	–	–	–	28/12	40	12.05 ± 2.74
IBIS Control	–	82	–	–	–	32/50	82	9.33 ± 1.69
IBIS-ASD	–	55	–	–	–	12/43	55	10.09 ± 1.62

2 Materials

2.1 Participants

Our study includes both a typical control population and a testing population with a neurodevelopmental condition. The control group comprises typically developing school-age children, selected from two large public datasets: the Adolescent Brain Cognitive Development (ABCD) Study and the Human Connectome Project Development (HCP-D) Study, assessed between 7-11 years of age. These datasets were filtered to ensure a representative inlier cohort. The Child Behavior Checklist (CBCL) [8] was used to exclude children with summary or subscale measures in the top 5% indicating behavioral issues. This selection resulted in a total of 1650 participants, 1485 were selected for training, and 165 were reserved for validation. The testing population was derived from the Infant Brain Imaging Study (IBIS), which examines autism spectrum disorder (ASD) in a population at high familial likelihood. 55 IBIS subjects with an ASD diagnosis were assessed between 7-12 years of age. Additionally, to mitigate domain shift effects, we selected an additional set of 82 low familial likelihood control participants, without a diagnosis of ASD, from IBIS for training and validation (Table 1).

Images were intensity-clipped to the 1st–99th percentiles, brain-masked using ANTsPyNet's deep-learning brain masking, and rigidly registered (T1w/T2w) to the MNI-152 1mm template using ANTs default settings. N4 bias correction and histogram matching (128 bins, 5 points, MNI-152) were applied. Background was cropped, intensities min–max normalized to [–1, 1]. T1w/T2w volumes treated as two-channel inputs to the U-Net–based denoising score-matching network. Behavioral measures such as the Differential Ability Scales-II (DAS-II) [5] and the Vineland Adaptive Behavior Scales-II (Vineland-II) [3] were used to assess cognitive and adaptive functioning. Additionally, the Autism Diagnostic Observation Schedule (ADOS) [7] was used to assess the severity of autism-related symptoms based on a clinician-administered semi-structured evaluation of social, communicative, and repetitive behaviors.

3 Method description

Figure 1 schematically illustrates the proposed framework. Via MSMA, feature embeddings are generated that captures atypicality. Via GHSOM, a manifold representing a morphospace of brain phenotypes is fit to these. Unseen atypical

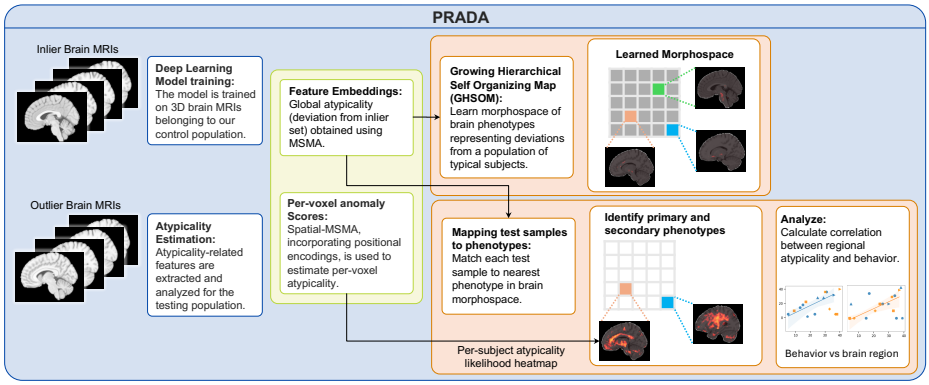

Fig. 1. Overview of the proposed framework for identifying brain atypicality patterns. An MSMA model is trained on inlier brain MRIs to compute a global atypicality. Per-voxel anomalies are estimated using spatial MSMA. A GHSOM learns a morphospace of brain phenotypes, mapping test samples to their closest phenotype. Primary and secondary phenotypes are identified, and correlations between regional atypicality and behavior are calculated.

data is then mapped into that morphospace to discover disorder phenotypes. Per-voxel atypicality quantification allows the generation of atypicality likelihood heatmaps and regional summaries for brain-behavior correlation analysis.

3.1 Machine Learning for Atypicality Detection

We use Multiscale Score Matching Analysis (MSMA), an unsupervised method that quantifies atypicality based on the norm of the score function—i.e., the gradient of the log-likelihood of the data distribution [12].

Multiscale Score Matching Analysis: MSMA builds on denoising score matching (DSM) by estimating score functions across multiple noise scales. Given a sample x, the score is defined as $s_\theta(x) = \nabla_x \log p_\theta(x)$, which measures deviations from typical data points. Instead of computing second-order derivatives, DSM approximates score matching using noisy samples. DSM objective is:

$$J_{\mathrm{DSM}}(\theta) = \mathbb{E}_{\tilde{x}\sim q_\sigma(x|\tilde{x}),x\sim p(x)}\left[\frac{1}{2}\|s_\theta(\tilde{x}) - \nabla_{\tilde{x}} \log q_\sigma(\tilde{x}|x)\|^2\right]. \tag{1}$$

MSMA extends DSM by incorporating multiple noise scales, allowing finer-grained atypicality detection. MSMA objective is:

$$J_{\mathrm{MSMA}}(\theta) = \sum_{l=1}^{L} w_l \mathbb{E}_{\tilde{x}\sim q_{\sigma_l},x\sim p(x)}\left[\frac{1}{2}\|s_\theta(\tilde{x},\sigma_l) - \nabla_{\tilde{x}} \log q_{\sigma_l}(\tilde{x}|x)\|^2\right]. \tag{2}$$

Spatial-MSMA Framework: Spatial-MSMA conditions the estimation of score norms on patch-wise spatial context. Given an image patch x_p, the model

estimates the log-likelihood of its score norm as $\log p_\theta(\|s(x_p)\| \mid z)$, where z encodes spatial metadata or global image features. This enables the model to associate atypicality with specific spatial locations, enhancing interpretability.

Atypicality maps: The patch-wise atypicality likelihood yields a voxel-wise atypicality map, which captures the likelihood of encountering the observed patch (with its shape, size, and intensity) at the given location conditioned on the rest of the image. This atypicality map can be visualized as a heatmap (see Fig 3). These heatmaps capture atypicality in the individual image space, but can be summarized across images via deformable registration into a prior template space with existing regional definitions. Here, we map individual atypicality maps into MNI-space and summarize regional atypicality within AAL regions by computing the median percentile atypicality relative to the distribution of typical data.

3.2 Structured Mapping of Brain Phenotypes

The Growing Hierarchical Self-Organizing Map (GHSOM) is a neural network model designed to adaptively represent the hierarchical structure of complex data. GHSOM dynamically adjusts its architecture during training, creating a multilayered structure to reflect data characteristics at various levels of detail [4].

The GHSOM begins with a single unit at level 0, representing the entire input space. The quantization error (QE) for this unit is computed as $\text{QE} = \frac{1}{N}\sum_{i=1}^{N}\|\mathbf{x}_i - \mathbf{w}\|$ where $\mathbf{x}_i$ are the input vectors, $\mathbf{w}$ is the model vector of the unit, and N is the total number of input samples. To determine the need for map expansion, the Mean Quantization Error (MQE) is calculated for each map as the average QE of its units: $\text{MQE} = \frac{1}{U}\sum_{u=1}^{U}\text{QE}_u$ where U is the number of units in the map. The local growing criterion ensures that individual units representing diverse subsets of data expand into new maps. A map grows if its MQE exceeds a fraction of the parent map's QE, scaled by w_l: $\text{MQE}_m > w_l \cdot \text{QE}_{\text{parent}}$. The global growing criterion is met if the QE of a unit exceeds a fraction of the QE at the top level, scaled by the parameter w_g: $\text{QE} > w_g \cdot \text{QE}_{(0)}$. The parameters w_g and w_l control the depth and granularity of the hierarchical structure, respectively. Smaller w_g values result in deeper hierarchies, while larger w_g values create more extensive maps at each level. In contrast, smaller w_l values lead to sparse maps, and larger w_l values promote deeper hierarchies.

When a unit satisfies the local growing criterion, a new map is initialized. The model vectors of the new units are initialized to maintain the topology of the parent map by averaging the neighboring units' vectors. The training process for each map uses the standard SOM procedure, followed by the insertion of additional rows or columns. The training process continues until all units meet the stopping criteria: $\text{MQE}_m \leq w_l \cdot \text{QE}_{\text{parent}}$ and $\text{QE} \leq w_g \cdot \text{QE}_{(0)}$. The overall framework of our PRADA approach is illustrated in Figure 1.

4 Results

MSMA and GHSOM were trained on typical subjects, and then atypical samples were mapped by assigning each to its nearest SOM unit, as shown in Fig. 2. w_l

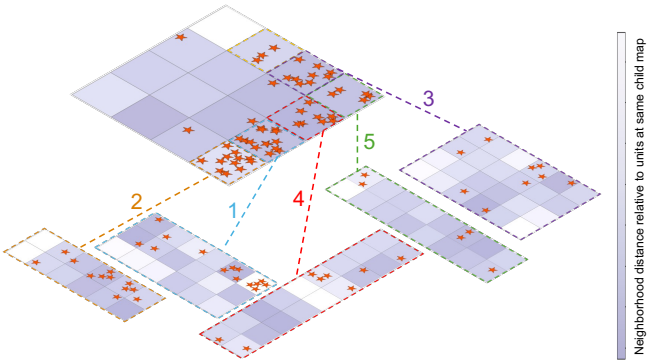

Fig. 2. Trained Growing Hierarchical Self-Organizing Map (GHSOM) for phenotype representation. The first level organizes primary phenotypes, while the second level refines each phenotype into more detailed subgroups. The GHSOM is trained using typical subjects, and atypical samples are overlaid by mapping each to its nearest unit. Red stars indicate ASD samples. Phenotypes are sorted by the number of ASD samples.

and w_g were 0.034 and 0.008, respectively, for consistent leaf node sample coverage. From the learned phenotype representations, we selected the two most-frequent SOM units for further analysis. These represent distinct ASD phenotypes with overlapping but also distinct patterns of atypicality as the atypicality percentile heatmaps in Fig. 3 illustrate. Each of these 2 phenotypes also captures significant correlations between regional brain atypicality and behavioral measures. While there is insufficient space here to discuss all observed associations, we highlighted some of the results below.

The first, most frequent ASD phenotype in our sample is characterized by structural brain atypicalities related to social-affective and sensory processing. We observed the strongest significant correlation between the CBCL-Social Problems Score and the left superior temporal gyrus atypicality ($R = 0.791$). The superior temporal gyrus is essential for language processing and social perception. The CBCL-Total Problems Score was associated with the left superior temporal gyrus ($R = 0.694$) and also the left posterior cingulate gyrus ($R = 0.702$), a region involved in self-referential thinking and social cognition [15, 27]. Other notable correlations include the ADOS-Derived Social Affect Total, assessed at an earlier age of 3 years, with the left posterior cingulate gyrus ($R = 0.764$) and right superior temporal gyrus ($R = 0.714$), reinforcing the role of these regions in social cognition [17]. Surprisingly, the CBCL-Attention Problems Score showed a negative correlation with the right Lobule VI of the cerebellar hemisphere ($R = -0.761$), indicating that also contrasting patterns of atypicality can be observed within a phenotype.

The second phenotype shows structural atypicality associations related to executive function and motor assessments. The strongest correlation was observed between the ADOS Restricted and Repetitive Behavior (RRB) Total measured at 3 years and the right superior parietal gyrus ($R = 0.946$). This region plays

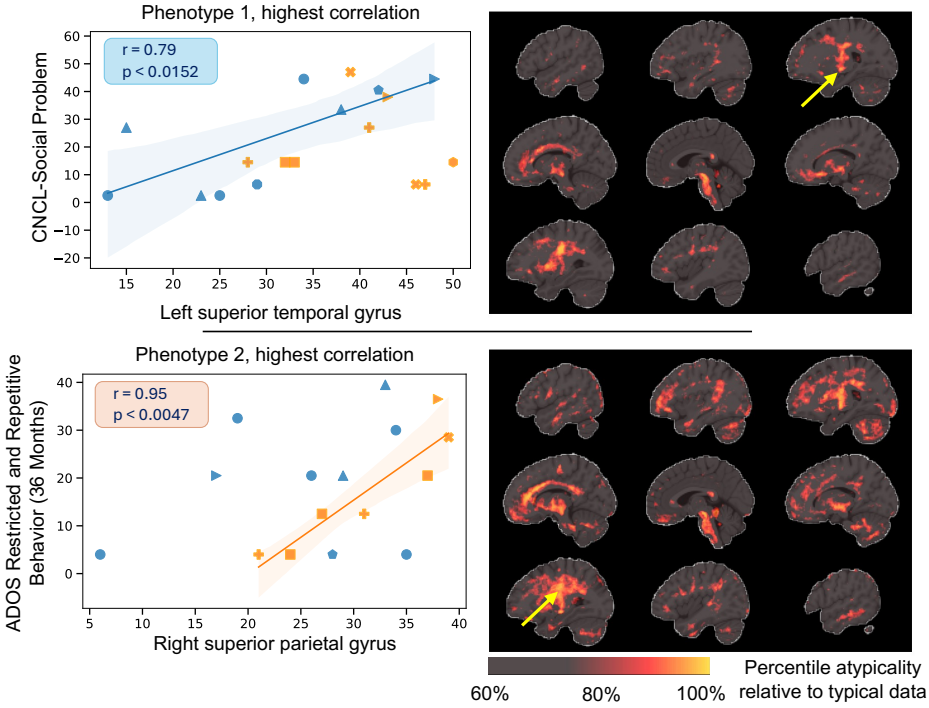

Fig. 3. Correlation between brain atypicality and behavioral measures for two primary phenotypes. Scatter plots show the strongest correlations for each phenotype (top: Phenotype 1/blue, bottom: Phenotype 2/orange) with both phenotypes plotted. Corresponding brain heatmaps display the median percentile atypicality relative to the distribution of typical data, with higher atypicality percentiles highlighted in red (80%) to yellow (100%). Yellow arrows indicate the plotted regions of interest.

a role in visuospatial and sensorimotor integration, functions that are often altered in ASD [17]. Significant correlations were also found between CBCL-Total Problems Score and the right inferior frontal gyrus, triangular part ($R = 0.917$), a region involved in response inhibition and executive control [23]. Other notable findings include correlations between the ADOS Restricted and Repetitive Behavior Total at 3 year and both the left thalamus ($R = 0.837$) and the left dorsolateral superior frontal gyrus ($R = 0.837$), regions associated with motor functioning. [17]. Additionally, CBCL-Thought Problems Score was linked to the right Crus II of the cerebellum ($R = 0.756$), reinforcing the cerebellum's involvement in ASD [25].

5 Conclusion

This work presents PRADA, a method for the exploration of structural phenotypes of neurodevelopmental disorders, here autism spectrum disorder, by

utilizing structural brain MRI data to identify image patterns of atypicality. Using score-based out-of-distribution quantification, SOM-based manifold & cluster learning approaches, PRADA identified two major ASD phenotypes with distinct structural associations between structural atypicality and behavioral traits. These phenotypes and their associations provide novel insights into potential mechanisms underlying ASD-related challenges.

For these phenotypes, we observed both overlapping and distinct structural regions of atypicality and associations with behavior and cognition. Phenotype 1 is characterized mainly by social-affective and sensory processing atypicality, whereas Phenotype 2 involves executive function and motor atypicality.

A limitation of our approach is the limited level of structural interpretability. While our framework provides the presence, locality, and degree of atypicality of brain structures, it does not indicate whether the detected atypicality is observed due to size, shape, or intensity effects at the observed location in the MR image.

While the study offers valuable insights, limitations include the test sample size, which may affect generalizability and the number of detectable brain phenotypes. Future work involves extending this approach to longitudinal and multimodal data, such as functional connectivity or genetics, and ablation studies to compare individual components of PRADA.

Disclosure of Interests. The authors have no competing interests to declare that are relevant to the content of this article.

References

1. Bergmann, P., Fauser, M., Sattlegger, D., Steger, C.: Uninformed students: Student-teacher anomaly detection with discriminative latent embeddings. In: Proceedings of the IEEE/CVF conference on computer vision and pattern recognition. pp. 4183–4192 (2020)
2. Cao, P., Wen, G., Liu, X., Yang, J., Zaiane, O.R.: Modeling the dynamic brain network representation for autism spectrum disorder diagnosis. Medical & Biological Engineering & Computing **60**(7), 1897–1913 (2022)
3. Community-University Partnership for the Study of Children, Youth, and Families: Review of the Vineland Adaptive Behavior Scales-Second Edition (Vineland-II). Edmonton, Alberta, Canada. (2011)
4. Coulson, M., Ferles, C., Winberg, S., Naidoo, K.J.: Growing hierarchical self-organising representation map (ghsorm). Information Sciences **642**, 119121 (2023)
5. Elliott, C.D., Hale, J.B., Fiorello, C.A., Dorvil, C., Moldovan, J.: Differential ability scales–ii prediction of reading performance: Global scores are not enough. Psychology in the Schools **47**(7), 698–720 (2010)
6. Gao, S., Mishne, G., Scheinost, D.: Nonlinear manifold learning in functional magnetic resonance imaging uncovers a low-dimensional space of brain dynamics. Human brain mapping **42**(14), 4510–4524 (2021)
7. Gotham, K., Pickles, A., Lord, C.: Standardizing ados scores for a measure of severity in autism spectrum disorders. Journal of autism and developmental disorders **39**, 693–705 (2009)

8. Hoffmann, W., Weber, L., König, U., Becker, K., Kamp-Becker, I.: The role of the cbcl in the assessment of autism spectrum disorders: An evaluation of symptom profiles and screening characteristics. Research in Autism Spectrum Disorders **27**, 44–53 (2016)
9. Katwal, S.B., Gore, J.C., Marois, R., Rogers, B.P.: Unsupervised spatiotemporal analysis of fmri data using graph-based visualizations of self-organizing maps. IEEE Transactions on Biomedical Engineering **60**(9), 2472–2483 (2013)
10. Li, M., Wang, Y., Tachibana, M., Rahman, S., Kagitani-Shimono, K.: Atypical structural connectivity of language networks in autism spectrum disorder: A meta-analysis of diffusion tensor imaging studies. Autism Research **15**(9), 1585–1602 (2022)
11. Li, Z., Li, J., Wang, N., Lv, Y., Zou, Q., Wang, J.: Single-subject cortical morphological brain networks: phenotypic associations and neurobiological substrates. NeuroImage **283**, 120434 (2023)
12. Mahmood, A., Oliva, J., Styner, M.: Multiscale score matching for out-of-distribution detection. arXiv preprint arXiv:2010.13132 (2020)
13. Mahmood, A., Oliva, J., Styner, M.: Localizing anomalies via multiscale score matching analysis. arXiv preprint arXiv:2407.00148 (2024)
14. Márquez-Caraveo, M.E., Rodríguez-Valentín, R., Pérez-Barrón, V., Vázquez-Salas, R.A., Sánchez-Ferrer, J.C., De Castro, F., Allen-Leigh, B., Lazcano-Ponce, E.: Children and adolescents with neurodevelopmental disorders show cognitive heterogeneity and require a person-centered approach. Scientific Reports **11**(1), 18463 (2021)
15. Pretzsch, C.M., Schäfer, T., Lombardo, M.V., Warrier, V., Mann, C., Bletsch, A., Chatham, C.H., Floris, D.L., Tillmann, J., Yousaf, A., et al.: Neurobiological correlates of change in adaptive behavior in autism. American Journal of Psychiatry **179**(5), 336–349 (2022)
16. Rauber, A., Merkl, D., Dittenbach, M.: The growing hierarchical self-organizing map: exploratory analysis of high-dimensional data. IEEE Transactions on Neural Networks **13**(6), 1331–1341 (2002)
17. Schipul, S.E., Keller, T.A., Just, M.A.: Inter-regional brain communication and its disturbance in autism. Frontiers in systems neuroscience **5**, 10 (2011)
18. Schirrmeister, R.T., Springenberg, J.T., Fiederer, L.D.J., Glasstetter, M., Eggensperger, K., Tangermann, M., Hutter, F., Burgard, W., Ball, T.: Deep learning with convolutional neural networks for eeg decoding and visualization. Human brain mapping **38**(11), 5391–5420 (2017)
19. Schlegl, T., Seeböck, P., Waldstein, S.M., Schmidt-Erfurth, U., Langs, G.: Unsupervised anomaly detection with generative adversarial networks to guide marker discovery. In: International conference on information processing in medical imaging. pp. 146–157. Springer (2017)
20. Selvaraju, R.R., Cogswell, M., Das, A., Vedantam, R., Parikh, D., Batra, D.: Grad-cam: Visual explanations from deep networks via gradient-based localization. In: Proceedings of the IEEE international conference on computer vision. pp. 618–626 (2017)
21. Taleb, H., Bokaei, M.H., Kani, D.H., Fard, F.R., Rafati, E., Nedaei, N.: Insurance of liability for self-driving cars. In: 2024 11th International Symposium on Telecommunications (IST). pp. 182–186. IEEE (2024)
22. Tye, C., Asherson, P., Ashwood, K.L., Azadi, B., Bolton, P., McLoughlin, G.: Attention and inhibition in children with asd, adhd and co-morbid asd+ adhd: an event-related potential study. Psychological medicine **44**(5), 1101–1116 (2014)

23. Uddin, L.Q.: Brain mechanisms supporting flexible cognition and behavior in adolescents with autism spectrum disorder. Biological Psychiatry **89**(2), 172–183 (2021)
24. Wang, Y., Huang, H., Rudin, C., Shaposhnik, Y.: Understanding how dimension reduction tools work: an empirical approach to deciphering t-sne, umap, trimap, and pacmap for data visualization. Journal of Machine Learning Research **22**(201), 1–73 (2021)
25. Wolff, J.J., Swanson, M.R., Elison, J.T., Gerig, G., Pruett, J.R., Styner, M.A., Vachet, C., Botteron, K.N., Dager, S.R., Estes, A.M., et al.: Neural circuitry at age 6 months associated with later repetitive behavior and sensory responsiveness in autism. Molecular autism **8**, 1–12 (2017)
26. Xu, X., Li, Y., Ding, N., Zang, Y., Sun, S., Shen, G., Song, X.: Quantitative assessment of brain structural abnormalities in children with autism spectrum disorder based on artificial intelligence automatic brain segmentation technology and machine learning methods. Psychiatry Research: Neuroimaging **345**, 111901 (2024)
27. Yasuhara, A.: Correlation between eeg abnormalities and symptoms of autism spectrum disorder (asd). Brain and Development **32**(10), 791–798 (2010)
28. Zerbi, V., Pagani, M., Markicevic, M., Matteoli, M., Pozzi, D., Fagiolini, M., Bozzi, Y., Galbusera, A., Scattoni, M.L., Provenzano, G., et al.: Brain mapping across 16 autism mouse models reveals a spectrum of functional connectivity subtypes. Molecular psychiatry **26**(12), 7610–7620 (2021)